IOPscience iopscience.iop.org

Home Search Collections Journals About Contact us My IOPscience

Tunnelling study on the temperature dependence of the band edge structure of SnTe

This article has been downloaded from IOPscience. Please scroll down to see the full text article.

1991 J. Phys.: Condens. Matter 3 3265

(http://iopscience.iop.org/0953-8984/3/19/005)

View the table of contents for this issue, or go to the journal homepage for more

Download details:
IP Address: 171.66.16.147
The article was downloaded on 11/05/2010 at 12:06

Please note that terms and conditions apply.

J. Phys.: Condens. Matter 3 (1991) 3265–3272. Printed in the UK

Tunnelling study on the temperature dependence of the band edge structure of SnTe

Hiroyuki Enomoto and Hajime Ozaki
Department of Electrical Engineering, Waseda University, Ohkubo 3-4-1, Shinjuku-ku, Tokyo 169, Japan

Received 19 December 1990

Abstract. The saddle-point-type band structure near the band edge of SnTe has been studied using tunnelling spectroscopy. Tunnelling measurements were performed on the single crystals of SnTe growth by the vapour phase transport method. The third derivative of the tunnelling current reflected the band edge structure peculiar to SnTe. We first observed the temperature dependence of the energy positions of the band edges and the saddle points of both the conduction and the valence bands separately in the temperature range between 120 and 150 K.

1. Introduction

SnTe is a narrow-gap semiconductor, known to have a special band edge structure [1–4]. The energy gap exists near the L point of the Brillouin zone. The details of the calculated band edge structure of SnTe is described as follows: the energy surface at the L point forms a saddle point, i.e. the valence band energy decreases as one moves away from the L point along the Λ axis but increases in the direction perpendicular to the Λ axis from the L point.

If the band edge structure of SnTe is the saddle point type, as described above, an interesting electronic behaviour, such as the negative resistance associated with the negative mass [5], is expected. The experimental study is thus expected to confirm the band edge structure of SnTe.

In 1973, Ota and Rabii [6] performed optical measurements on epitaxially grown thin films of SnTe. They found two kinks in the carrier concentration dependence of the optical absorption edge. They concluded that these two kinks resulted from the band edge and the saddle point. In the optical measurements, however, there is some arbitrariness in the determination of the absorption edge because of the free-carrier absorption. The optical absorption measurements elucidate the joint density of states of the conduction and valence bands but cannot give those structures separately.

On the other hand, the tunnelling measurements can detect the conduction and valence band edge structures directly and separately [7]. In our previous study [8], we performed tunnelling measurements and detected the band edges and the saddle points in the conduction and the valence band of epitaxially grown SnTe films. In this paper, we have advanced the study, using bulk crystals prepared by the vapour transport

method, and obtained the temperature dependence of the energy separations of these band structures in the temperature range between 120 and 150 K.

2. Experimental details

2.1. Crystal growth

Single crystals of SnTe were prepared by using the vapour transport method. Source materials of 99.99% pure Sn and 99.99% pure Te in stoichiometric amounts were sealed into the quartz ampoules under a vacuum of 4×10^{-4} Pa together with excess Sn in order to reduce Sn vacancies. The ampoules were first heated to 840 °C in the electrical furnace for 10 h so that reaction occurred. Then the temperature gradient was set to -5 °C cm^{-1}, and the well reacted source materials were transferred to the cooler region in the ampoules as a vapour. After growth for 24 h, the SnTe single crystals became about 3 mm × 3 mm × 2 mm in size.

Because the narrow region of the compound SnTe lies in the Te-rich region in the Sn–Te binary alloy [9], all samples of SnTe behave as the heavily degenerated p-type semiconductors owing to the Sn vacancies. The Hall measurements showed the carrier concentration of our crystals ranged between 0.7×10^{20} and 3.0×10^{20} cm^{-3}.

2.2. Junction fabrication

In order to fabricate the tunnel junctions, Al_2O_3/Al plates were prepared. An Al film 300 nm thick was evaporated onto the glass substrate in a vacuum of 4×10^{-4} Pa. After the vacuum evaporation, the Al film surface was oxidized in an O_2 atmosphere at 4 Pa for 30 min at 80 °C. The thickness of the oxide layer was about 5 nm.

The tunnel junction was fabricated using the planar contact technique [10, 11]. This tunnel junction is more stable against the temperature change than the point contact tunnel junction with the oxidized Ta wire adopted in our previous study [8]. The geometry of the planar contact tunnel junction is shown in figure 1. The as-grown SnTe(100) surface was softly pressed to the surface of the Al_2O_3/Al plate. In order to get a good ohmic contact to the counter-electrode, the back-side surface of the sample was roughly lapped by the SiC grade 2000 powders. It was also confirmed that the voltage drop across the series resistance, which affects the use of the bias scale as an energy scale, was small enough (less than 1 Ω) compared with the tunnel junction resistance (about 100 Ω). A stabilizer, as shown in figure 1(*b*), was used on top of the sample in order to get a stable junction and also to transmit the pressure uniformly from the phosphor bronze spring in figure 1(*a*).

2.3. Tunnelling measurement

Tunnelling measurements were performed using the standard AC modulation method. In this study, the modulation bias was 2 mV (RMS) and the modulation frequency was 1 kHz. In order to detect a fine structure in the density of states, a lower temperature is advantageous for the tunnelling measurements. However, SnTe causes a phase transition from the NaCl structure to the rhombohedral structure [12], whose transition temperature is strongly dependent on the carrier concentration. Below the phase transition temperature, the band edge structure of SnTe is no longer considered to be the

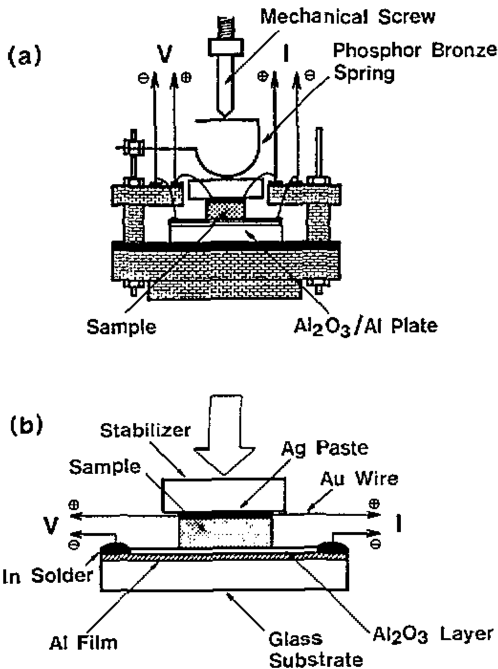

Figure 1. Planar contact tunnel junction: (a) sketch of the whole unit; (b) the core unit. To fabricate the tunnel junction, the as-grown crystal surface of the sample is softly pressed onto the surface of the Al_2O_3/Al plate. The pressure is controlled by the mechanical screw and the phosphor bronze spring.

saddle point type. Moreover, the tunnel barrier of Al_2O_3 layer is broken by the structural change of SnTe, when the temperature goes through the phase transition temperature. We must thus perform the tunnelling measurements somewhat above the phase transition temperature, which is estimated as 80–110 K from the carrier concentration of our samples.

To perform the tunnelling measurements at such a higher temperature as described above, we have employed a higher derivative of the tunnelling current to improve the separation of the very weak band-structure-related peaks from the background features. When the tunnelling current is masked by other currents, such as the space-charge-limited current which flows over the tunnel barrier or the hopping conduction in the insulator, we can see no structures, which reflect the density of states, in the I–V and even in the $\mathrm{d}I/\mathrm{d}V$–V characteristics. Thus, only by taking a higher derivative of the current, can we detect such structures. For example, at a bias position where the slope of the $\mathrm{d}I/\mathrm{d}V$–V curve changes, a step can be seen in the $\mathrm{d}^2 I/\mathrm{d}V^2$–$V$ curve, and a spike in the $\mathrm{d}^3 I/\mathrm{d}V^3$–$V$ curve. So, a small change in the density of states becomes more distinctive in the higher derivatives of the current. As shown in our model calculation [8], all structures of the density of states at the band edges and the saddle points of SnTe appear as spikes in the $\mathrm{d}^3 I/\mathrm{d}V^3$–$V$ curve.

3. Results and discussion

Figure 2 shows one of the tunnelling characteristics measured at 121 K. The positive-bias side corresponds to the conduction band side of SnTe. No structures could be detected in the I–V, $\mathrm{d}I/\mathrm{d}V$–V and $\mathrm{d}^2 I/\mathrm{d}V^2$–$V$ curves because of the thermal noise and

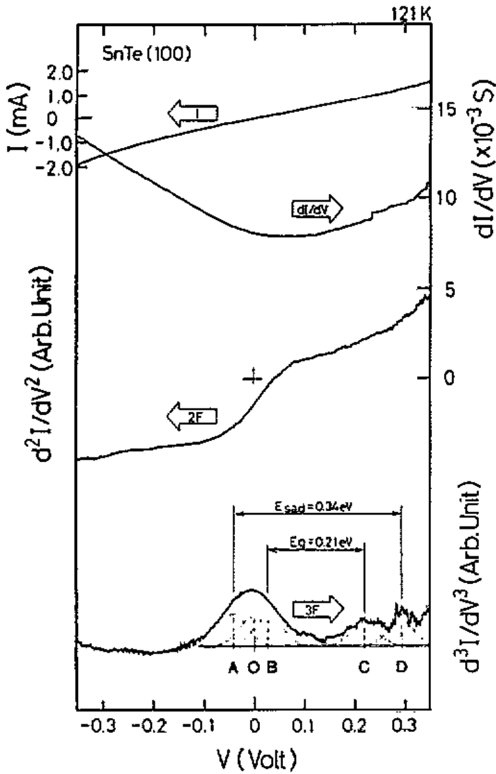

Figure 2. Tunnelling spectra of the single crystal of SnTe measured at 121 K. In the third-derivative curve (d^3I/dV^3–V), the dotted curves denote the decomposed components originating from the band edges and the saddle points.

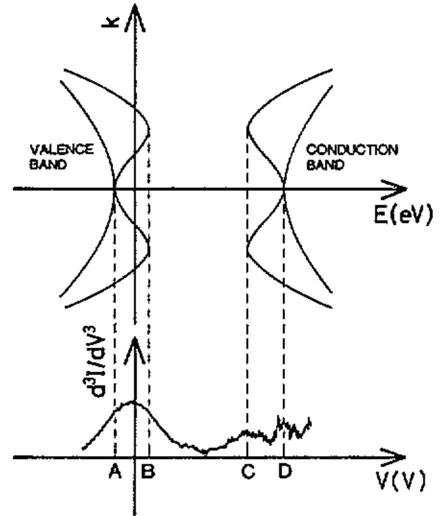

Figure 3. Schematic energy relation between the third-derivative curve and the energy band of SnTe.

the broadening of the carrier energy distributions. In the d^3I/dV^3–V curve in figure 2, however, one large broad peak can be seen near the Fermi level (zero bias) and some peaks on the conduction band side. These peaks also contain noise due to thermal fluctuation at the measuring temperature and to the instability of the tunnel junction at a higher bias. Compared with several other d^3I/dV^3–V curves measured at the same temperature, however, we could detect two peaks C and D which surely appear at the same bias positions. We consider that they are derived from the band edge and the saddle point in the conduction band of SnTe, because their energy separation is almost equal to the theoretical value [2, 3]. Referring to the theoretical value of the temperature-dependent energy gap of SnTe [2, 13], we know that the energy positions of the band edge and the saddle point in the valence band are located near zero bias. The large broad peak near zero bias has two shoulders on each side, and the separation of these shoulders corresponds to the theoretical energy separation of the band edge and the saddle point in the valence band [2, 3]. Peak decomposition was performed using three peaks with the assumption that the peak widths of A, B, C and D are the same. If a current component with the bias dependence of $I \propto V^2$, such as a space-charge-limited current, flows over the tunnel barrier, a peak will appear at zero bias in the d^3I/dV^3–V curve [8],

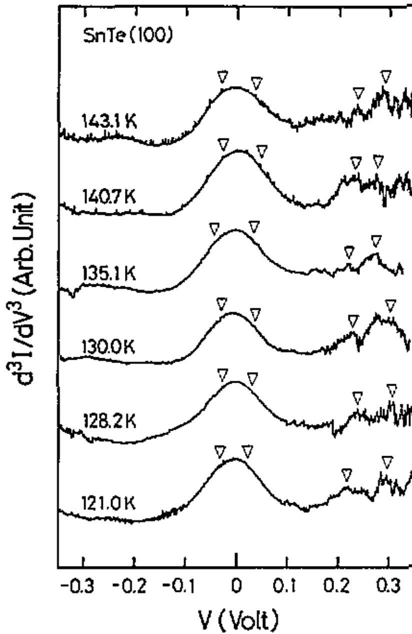

Figure 4. Temperature dependence of the d^3I/dV^3–V curves. The open inverted triangles indicate the energy positions of each component of figure 2, which are determined from repeated measurements at the same temperature.

i.e. peak O in figure 2. The peak positions of A and B and the peak width of O were estimated by the best fitting of the decomposed peaks to the experimental curve. As there is close similarity between the peak positions of A, B, C and D and the calculated energy separations of the band edges and the saddle points in the conduction and the valence bands [2, 3], we attribute these peaks to the singular points of the band structure, as shown in figure 3. Compared with our previous study [8], peak C is much less pronounced in the present study; this might be due to the difference in the crystallinity at the surface which depends on the crystal growth technique. The Fermi level thus lies in the valence band, which is consistent with the temperature dependence of the resistivity of the sample, but is slightly higher than that calculated [2] from the carrier concentration of the sample. The difference will be due to the pinning of the Fermi level at the surface of SnTe.

Figure 4 shows the temperature dependence of the d^3I/dV^3–V curves for the same sample as in figure 2. The open inverted triangles in figure 4 show the positions where peaks appear commonly in the repeated measurements at each temperature. The temperature dependences of the energy positions of these open inverted triangles in figure 4 are plotted in figure 5. Each plot means separate samples, and the open triangles in figure 5 correspond to the sample shown in figures 2 and 4. The temperature dependences are not clear in figure 5, because of the differences between the Fermi levels of the samples. To eliminate the scattering of the plots due to the difference between the Fermi levels, the temperature dependences of the energy separations E_g between the band edges and the energy separations E_{sad} between the saddle points, are shown in figure 6. In this figure, the full straight lines are the least squares of the experimental plots. In the temperature region from 120 to 150 K, E_g and E_{sad} have small negative coefficients, which is consistent with the theoretical result [13]. The broken lines in the figure are the interpolated straight lines between the calculated values at 0 and 400 K [13]. The values

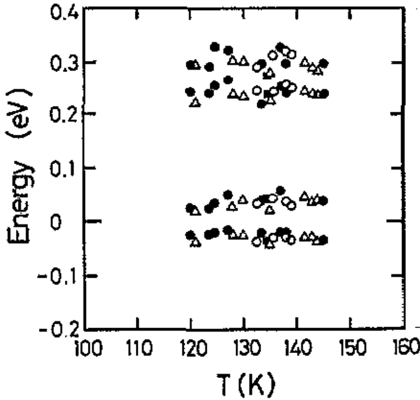

Figure 5. Temperature dependences of the energy positions of each open inverted triangle in figure 4, including the data from other samples. O: E870612C(100), $p \simeq 7.6 \times 10^{19}$ cm^{-3}; ●: E870612C(111), $p \simeq 7.6 \times 10^{19}$ cm^{-3}; △: E870812A(100), $p \simeq 1.3 \times 10^{20}$ cm^{-3}; ■: E870420A(111), $p \simeq 1.5 \times 10^{20}$ cm^{-3}.

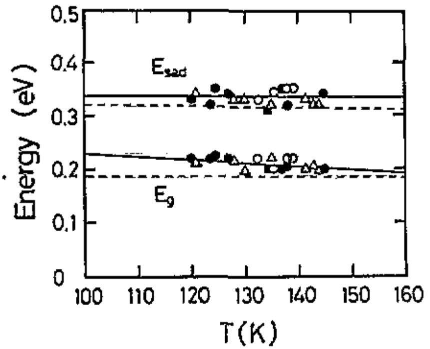

Figure 6. Temperature dependences of the energy separations E_g of the band edges and the energy separations E_{sad} of the saddle points: ———, least squares of the experimental plots; – – –, interpolated straight lines between the calculated values at 0 and 400 K [13]. O: E870612C(100), $p \simeq 7.6 \times 10^{19}$ cm^{-3}; ●: E870612C(111), $p \simeq 7.6 \times 10^{19}$ cm^{-3}; △: E870812A(100), $p \simeq 1.3 \times 10^{20}$ cm^{-3}; ■: E870420A(111), $p \simeq 1.5 \times 10^{20}$ cm^{-3}.

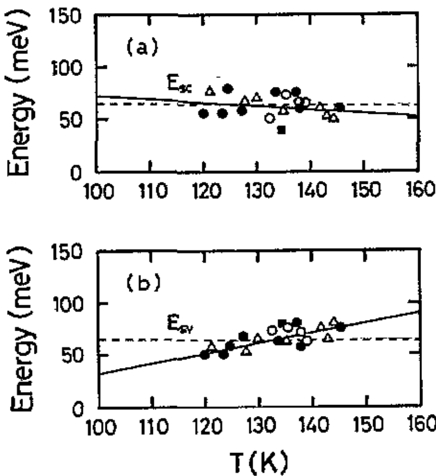

Figure 7. Temperature dependences of (*a*) the energy separations E_{sc} between the band edge and the saddle point in the conduction band and (*b*) the energy separations E_{sv} between the band edge and the saddle point in the valence band: ———, least squares of the experimental plots; – – –, lines interpolated as in figure 6. O: E870612C(100), $p \simeq 7.6 \times 10^{19}$ cm^{-3}; ●: E870612C(111), $p \simeq 7.6 \times 10^{19}$ cm^{-3}; △: E870812A(100), $p \simeq 1.3 \times 10^{20}$ cm^{-3}; ■: E870420A(111), $p \simeq 1.5 \times 10^{20}$ cm^{-3}.

of E_g and E_{sad} obtained in this study are consistent with those obtained by optical measurements at room temperature [6].

Figure 7(*a*) shows the temperature dependence of the energy separation E_{sc} between the band edge and the saddle point in the conduction band and figure 7(*b*) shows the energy separation E_{sv} in the valence band. The full lines are the least squares of the experimental plots, and the broken lines are those interpolated as in figure 6. The value of E_{sc} is somewhat smaller than that obtained previously in the epitaxial film grown on

Table 1. The least squares of E_g, E_{sad}, E_{sc} and E_{sv}.

Temperature (K)	Energy (eV)			
	E_g	E_{sad}	E_{sc}	E_{sv}
120	0.334	0.216	0.065	0.053
150	0.334	0.197	0.055	0.081

the KCl substrate [8]. Figure 7 shows that the temperature dependence of E_{sc} is rather small, while E_{sv} has an appreciable positive temperature coefficient. The least squares of E_g, E_{sad}, E_{sc} and E_{sv} at 120 and 150 K, obtained in this study, are listed in table 1.

4. Conclusion

We have investigated the saddle-point-type band structure near the band edge of SnTe using tunnelling spectroscopy. Employing the third derivative of the tunnelling current, we could detect the band edge structure peculiar to SnTe. The temperature dependences of the energy positions of the band edges and the saddle points of both the conduction and the valence bands were firstly observed in the temperature range between 120 and 150 K. The temperature dependence of E_{sc} is rather small, while E_{sv} has an appreciable positive temperature coefficient.

Acknowledgments

The authors would like to thank Mr M Baba, Mr N Andoh and Mr K Mutoh for their help in the sample preparation. We would also like to thank Mr S Oguro and Mr K Haga for their kind assistance with the tunnelling measurements. We are indebted to Mr Y Miyamoto for his helpful discussion.

References

[1] Tung Y W and Cohen M L 1969 *Phys. Lett.* **29A** 236
[2] Cohen M L and Tsang Y W 1970 *The Physics of Semimetals and Narrow-Gap Semiconductors* (Oxford: Pergamon) p 303
[3] Rabii S 1969 *Phys. Rev.* **182** 821
[4] Ota Y and Rabii S 1970 *The Physics of Semimetals and Narrow-Gap Semiconductors* (Oxford: Pergamon) p 343
[5] Krömer H 1959 *Proc. IRE* **5** 397
[6] Ota Y and Rabii S 1973 *J. Nonmet.* **1** 117
[7] Esaki L 1966 *J. Phys. Soc. Japan* **21** 589 suppl.
[8] Miyamoto Y, Enomoto H and Ozaki H 1989 *J. Phys. Soc. Japan* **58** 2092
[9] Shunk F A 1969 *Constitution of Binary Alloys, Second Supplement* (New York: McGraw-Hill) p 688
[10] Ozaki H, Ohara T, Fujimoto H and Hotchi H 1985 *Charge Density Waves in Solids* (Berlin: Springer) p 141
[11] Enomoto H, Gotoh K, Iida K, Takano Y, Mori N and Ozaki H 1988 *High-Temperature Superconductors II (Mater. Res. Soc. Symp. Proc. 99)* (Pittsburgh, PA: Materials Research Society) p 853

[12] Jantsch W 1983 *Dynamical Properties of IV–VI Compounds* (Berlin: Springer) p 1
[13] Tsang Y W and Cohen M L 1971 *Phys. Rev.* B 3 1254